Ionics (2020) 26:3769–3775
https://doi.org/10.1007/s11581-020-03570-0

ORIGINAL PAPER

# Preparation and electrochemical properties of cationic substitution $Li_2Mn_{0.98}M_{0.02}SiO_4$ (M = Mg, Ni, Cr) as cathode material for lithium-ion batteries

Luoxuan Wang[1,2,3] · Yang Zhan[1,2,3] · Shao-hua Luo[1,2,3,4] · Yafeng Wang[1,2,3] · Si Li[3] · Longjiao Chang[5]

Received: 27 March 2020 / Accepted: 5 April 2020 / Published online: 24 April 2020


## Abstract

$Li_2Mn_{0.98}M_{0.02}SiO_4$ (M = Mg, Ni, Cr) cathode material for lithium-ion batteries was synthesized by traditional solid-phase doping method used $Li_2CO_3$, $MnCO_3$, $(C_2H_5O)_4Si$, and $MgC_2O_4{\cdot}2H_2O$ (or $NiC_2O_4{\cdot}2H_2O$ or $C_2O_3$) as staring materials. The suitable calcination temperature (700 °C) was obtained by TG-DTA curve. The influence of different doping amount on the crystal structure, micromorphology, and electrochemical properties of $Li_2MnSiO_4$ was studied by XRD, SEM, and electrochemical performance measurement. The XRD patterns indicate that the $Li_2MnSiO_4$ crystallized in an orthorhombic structure with a space group of $Pmn2_1$. It can be seen from SEM images that Mg doping has no effect on the micromorphology, Cr doping can refine the powder, and the particle size is about 200–800 nm. The electrochemical performance measurement demonstrates that the $Li_2Mn_{0.98}Cr_{0.02}SiO_4$ shows the best electrochemical performance with an initial discharge capacity of 29.8 mAh $g^{-1}$ at 0.1 C, and the discharge capacity retention rate after 70 cycles is 20.1%.

**Keywords** Lithium-ion batteries · Cathode material · $Li_2Mn_{0.98}M_{0.02}SiO_4$ (M = Mg, Ni, Cr) · Solid-phase doping method

## Introduction

Lithium-ion batteries (LIBs) are widely used in a variety of portable electronic products and will be widely used in the electric vehicle and hybrid vehicle industry [1–3]. Padhi et al. [4] reported for the first time that $LiFePO_4$, a phosphate compound with olivine structure, has high capacity, good cycling performance, safety, low cost, and environmental friendliness. Recently, the $Li_2MSiO_4$ (M = Mn, Fe, Co, Ni) series, which is isomorphic with $LiFePO_4$, has also attracted people's attention [5, 6]. Among them, the theoretical voltage platform of $Li_2MnSiO_4$ is about 4.1 V, which is equivalent to the voltage platform of $LiCoO_2$ (3.9–4.0 V). It is suitable for the current battery system and maybe a cheap green electrode material to replace $LiCoO_2$ in the future [7–9]. R. Dominiko et al. [10] synthesized $Li_2MnSiO_4$ by the improved Pechini method, but the material has the disadvantages of small specific capacity, poor cycle performance, and poor conductivity [5]. Therefore, material modification is necessary.

At present, the main methods of surface modification of $Li_2MnSiO_4$ are carbon coating [7, 11, 12] and metal doping. The theoretical capacity of $Li_2MnSiO_4$ can reach 333 mAh $g^{-1}$, and the first voltage platform is about 4.1 V [10]. Gong et al. [13] have synthesized the $Li_2Mn_{1-x}Mg_xSiO_4$/C ($x$ = 0–0.3) cathode by the sol-gel method in orthorhombic $Pmn2_1$ form. The Mg doping improved the specific capacity of $Li_2MnSiO_4$ up to 229 mAh $g^{-1}$. Deng H et al. [14] believe that the substitution of Ni has some effect on the preparation of pure phase, grain refinement, increase of discharge capacity, decrease of resistivity, and increase of diffusion coefficient of lithium ion. Cheng H M et al. [15] found that $Li_2Mn_{92.5\%}Cr_{7.5\%}SiO_4$/C significantly improved the cycle

✉ Shao-hua Luo
tianyanglsh@163.com

✉ Longjiao Chang
jsz337@sina.com

1 School of Materials Science and Engineering, Northeastern University, Shenyang 110819, People's Republic of China

2 Key Laboratory of Dielectric and Electrolyte Functional Material Hebei Province, Qinhuangdao, People's Republic of China

3 School of Resources and Materials, Northeastern University at Qinhuangdao, Qinhuangdao 066004, People's Republic of China

4 State Key Laboratory of Rolling and Automation, Northeastern University, Shenyang 110819, People's Republic of China

5 School of New Energy, Bohai University, Jinzhou 121013, People's Republic of China

stability and discharge capacity. Its initial discharge capacity can reach 255 mAh $g^{-1}$. After 50 cycles, the discharge capacity is still around 60 mAh $g^{-1}$.

In this work, we have successfully prepared $Li_2Mn_{0.98}M_{0.02}SiO_4$ (M = Mg, Ni, Cr) by the solid-phase method to modify $Li_2MnSiO_4$ samples. The effect of metal (Mg, Ni, Cr) doping on $Li_2MnSiO_4$ was evaluated by XRD, SEM, and electrochemical performance measurement.

## Experimental

### Material preparation

$Li_2Mn_{0.98}M_{0.02}SiO_4$ (M = Mg, Ni, Cr) was synthesized by solid-phase doping, and its preparation process is illustrated in Fig. 1. Using deionized water as the dispersant, the raw materials $Li_2CO_3$, $MnCO_3$, $(C_2H_5O)_4Si$, and $MgC_2O_4 \cdot 2H_2O$ (or $NiC_2O_4 \cdot 2H_2O$ or $C_2O_3$) were weighed according to the amount ratio of certain substances, in which Li:Mn:M:Si = 2:0.98:0.02:1 (M = Mg, Ni, Cr). The raw materials were dissolved in deionized water to form a uniform solution and milled for 5 h can get the liquid mixture, which would be drying in a drying oven at 80 °C, then sieved it with 100 mesh screen mesh to obtain the mixed raw material. Put the mixed raw material in the tubular furnace and calcined at 400 °C for 8 h, then sieved with 100 mesh screen mesh, the precalcined material was obtained. The precalcined material was placed in the tubular furnace and calcined at 700 °C for 8 h, sieving with 200 mesh screen mesh to obtain the final calcined $Li_2MnSiO_4$ cathode material doped with different metals.

### Material characterization

TG-DTA is a common method to study phase diagram and phase transformation. We use TG and DTA to get the best calcination temperature [16]. Thermogravimetric analysis of the precursor was recorded by the thermogravimetry and differential thermal analysis (TG-DTA, HCT-2) at a heating speed of 10 °C $min^{-1}$ from 20 to 800 °C in argon. The X-ray diffraction analyzer used in this paper is DX-2500. The phase and crystal properties of the material are analyzed under the condition of 30 kV and 25 mA. The scanning electron microscope used in this paper is SSX-550. In order to increase the conductivity of the sample surface, the sample was sprayed with gold before the experiment to obtain the best observation effect.

### Electrochemical measurements

The positive electrode was composed of 75% active substance, 17% conductive carbon black and 8% polyvinylidene fluoride (PVDF). *N*-methyl-2-pyrrolidinone (NMP) was added to make a slurry with a certain fluidity, which was evenly coated on the aluminum foil, dried at 80 °C, and then rolled on the roller press to make the electrode smooth, compact, and flat. Place the electrode flat in a vacuum drying oven at 80–100 °C and bear heavy pressure. The processed electrode was cut into disks with a diameter of 10 mm as a spare electrode. The electrolyte was mixed with 1 mol/L $LiPF_6$ EC:DMC (1:1) (Beijing Chemical Reagent Research Institute). The separator was Celgard 2400, and the metal lithium sheet was used as the negative electrode. The CR2032 button battery was packaged in the glove box filled with argon. Galvanostatic charge and discharge tests were performed

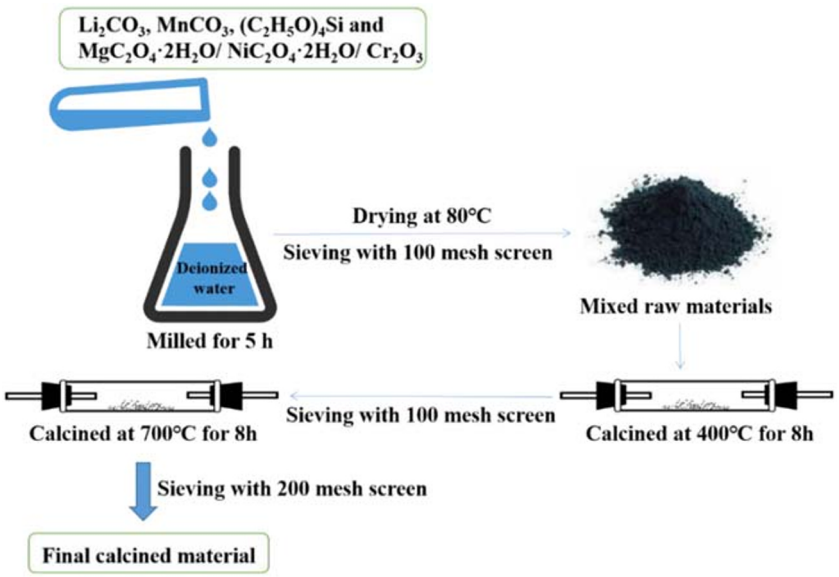


**Fig. 1** Schematic diagram of $Li_2Mn_{0.98}M_{0.02}SiO_4$ (M = Mg, Ni, Cr) preparation process

using a battery test system (LAND, CT2001A made by China) between 1.5 and 4.8 V, the current density was 0.1 C, and the test temperature was room temperature. Cyclic voltammetry (CV) was performed on a CHI660C electrochemical analyzer (Chenhua, China) at a scanning rate of 0.05 mV $s^{-1}$.

## Results and discussion

The preparation temperature has a great influence on the crystallization and structural properties of the material, so it is necessary to study the appropriate calcination temperature to prepare $Li_2MnSiO_4$, in order to make its electrochemical performance better. TG-DTA measurement is carried out to study the thermal stability of $Li_2MnSiO_4$ under air atmosphere [17–19]. The thermogravimetry of the precursor mixture is carried out in $N_2$ atmosphere; the TG-DTA curve is shown in Fig. 2. The heating rate is 10 °C $min^{-1}$, and the gas flow rate of $N_2$ is 30 mL $min^{-1}$.

The total reaction equation of $Li_2MnSiO_4$ powders synthesized with $Li_2CO_3$, $MnCO_3$ and $(C_2H_5O)_4Si$ as precursors can be expressed as follows:

$$Li_2CO_3 + MnCO_3 + (C_2H_5O)_4Si \rightarrow^{N_2} Li_2MnSiO_4 + \text{else} \quad (1)$$

According to the mass change before and after the reaction, the loss on ignition rate can be calculated as follows:

$$\text{Ignition loss} = 1 - \text{Productivily} = 1 - \frac{160.906}{73.8 + 114.95 + 208.33} \approx 60\% \quad (2)$$

Consistent with the weight loss in Fig. 2.

The dispersive endothermic peak of precursor mixture at 75–150 °C is the volatilization of organic matter in TEOS, which is lighter in weight and less in weight loss curve. It decomposes when the temperature is higher than the atmospheric temperature, and the decomposition speed increases with the increase of temperature. There is a large degree of weight loss near 300–650 °C, and there are different intensity endothermic peaks on the DTA curve. It can be seen from the DTA curve that there are obvious weight loss processes at 387 °C and 640 °C, corresponding to the decomposition of the mixed raw materials. After 690 °C, TG and DTA curves do not show obvious weight loss and heat absorption and exothermic peak (curve burr was a noise of testing instrument). This shows that when the temperature is higher than 700 °C, the decomposition of the precursor is completed, and $Li_2MnSiO_4$ is basically completed. Therefore, 700 °C is selected as the minimum calcination temperature.

Figure 3 shows the XRD patterns of $Li_2Mn_{0.98}M_{0.02}SiO_4$ (M = Mg, Ni, Cr). From Fig. 3, we can see that the main peaks of $Li_2MnSiO_4$ and $Li_2Mn_{0.98}M_{0.02}SiO_4$ (M = Mg, Ni, Cr) samples correspond to the $Li_2MnSiO_4$ phase of orthogonal structure, the space group is $Pmn2_1$, and the five main diffraction peaks correspond to (010), (011), (111), (210), and (002) crystal faces, respectively, which indicates that the doped metal atoms have successfully dissolved into the $Li_2MnSiO_4$ lattice.

Compared with the JCPDS standard card (75-7861), the undoped $Li_2MnSiO_4$ sample has MnO impurity phase. With Mg and Ni doping into $Li_2MnSiO_4$ sample, the peak value of MnO diffraction increases. Different from $Li_2Mn_{0.98}Ni_{0.02}SiO_4$ sample, the main diffraction peak intensity of $Li_2Mn_{0.98}Mg_{0.02}SiO_4$ sample decreases, which shows

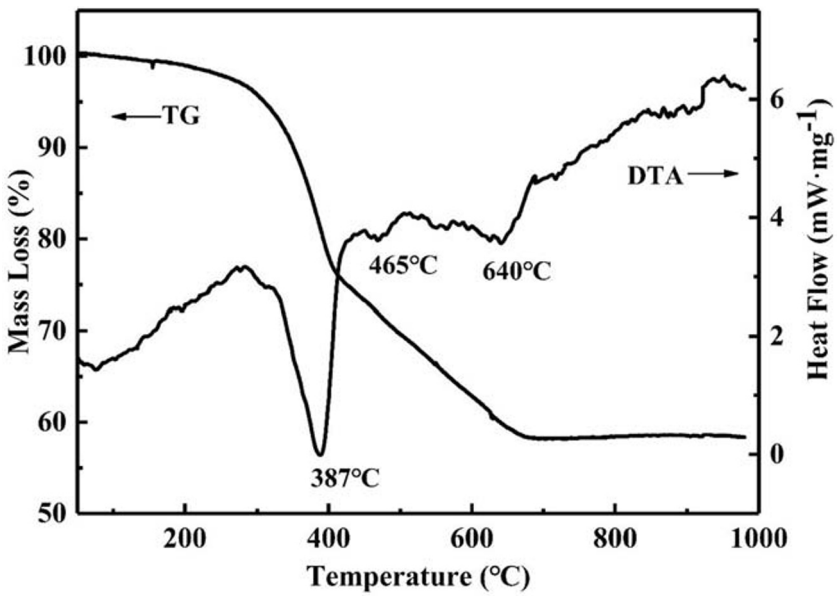


**Fig. 2** TG-DTA curve of the mixture of $MnCO_3$, $Li_2CO_3$ and $(C_2H_5O)_4Si$

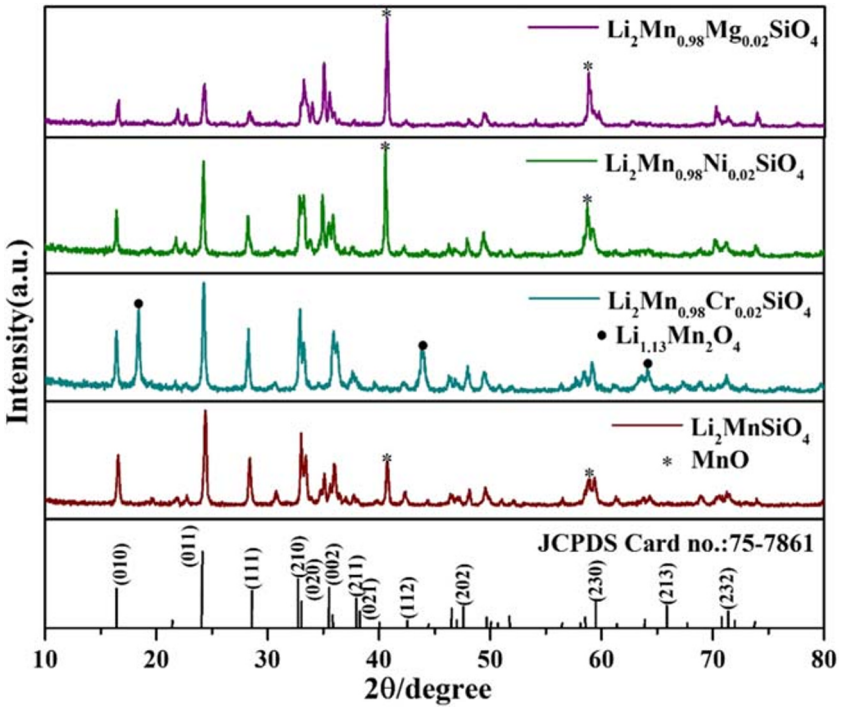


**Fig. 3** XRD patterns of $Li_2Mn_{0.98}M_{0.02}SiO_4$ (M = Mg, Ni, Cr) samples

that Mg doping has no effect on the enhancement of crystallinity, but it may also be related to Mg doping amount. However, in $Li_2Mn_{0.98}Cr_{0.02}SiO_4$ sample, the MnO impurity phase diffraction peak disappeared gradually, and the new diffraction peaks appeared near $2\theta$ value of 18°, 44°, and 65°, respectively. According to the analysis, $Li_{1.13}Mn_2O_4$ is produced. Because $Li_{1.13}Mn_2O_4$ can be used as a positive electrode material of battery and has excellent electrochemical performance, the electrochemical performance of $Li_2MnSiO_4$ will be greatly improved [20].

Figure 4 is the SEM of $Li_2MnSiO_4$ and $Li_2Mn_{0.98}M_{0.02}SiO_4$ (M = Mg, Ni, Cr) samples. It can be seen from the figure that the crystal growth of undoped $Li_2MnSiO_4$ is complete, and the particles are relatively large. Most of the primary particles gather together and gather into the secondary particles of large particles. The particle morphology of $Li_2Mn_{0.98}Mg_{0.02}SiO_4$ sample (Fig. 4b) and $Li_2MnSiO_4$ sample (Fig. 4a) is similar, and the maximum particle size of the two samples can reach 3000 nm, which shows that Mg doping has no significant effect on the microstructure of $Li_2MnSiO_4$. From Fig. 4c, it can be seen that the crystal surface of $Li_2Mn_{0.98}Ni_{0.02}SiO_4$ sample appears tiny particles and gradually becomes larger, and the particle morphology tends to be regular, and the crystallinity gradually increases. Figure 4 d is the SEM of $Li_2Mn_{0.98}Cr_{0.02}SiO_4$ sample. We can see that many particles still maintain the primary particle shape, and the maximum size is basically 1100 nm, far less than Mg ion and Ni ion doping. This shows that the size of the particles is reduced and the diffusion property of the ions in $Li_2MnSiO_4$ crystal is improved. The larger the size of the crystal, the

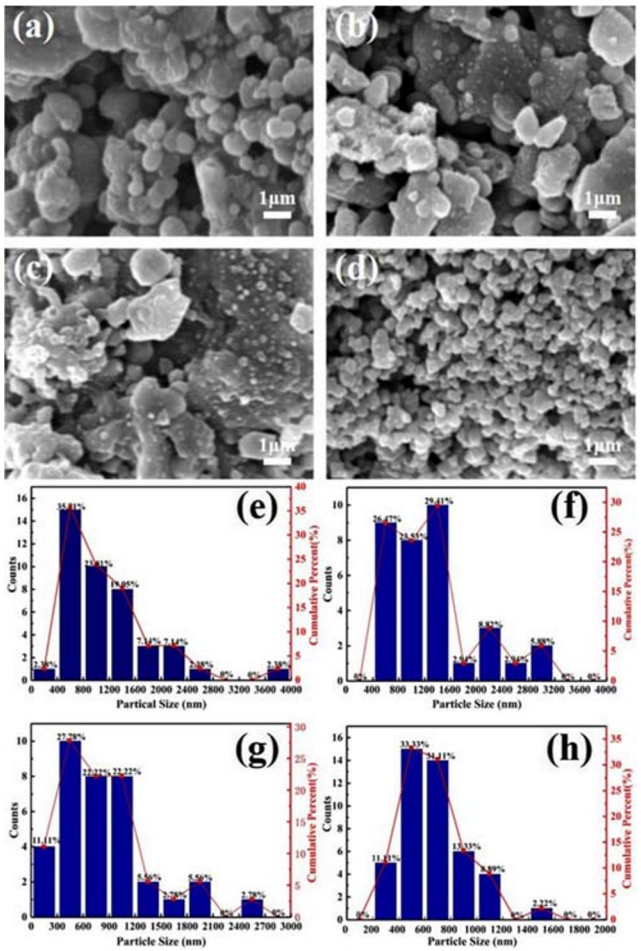


**Fig. 4** SEM images of **a** $Li_2MnSiO_4$ and **b**–**d** $Li_2Mn_{0.98}M_{0.02}SiO_4$ (M = Mg, Ni, Cr) samples were particle size summary figures (**e**–**h**)

longer the distance of $Li^+$ diffusion in the solid phase, and the more limited the electrical properties of the material are. Therefore, the reduction of particle size is helpful to the development of the specific capacity of materials.

Figure 5 shows the first charge and discharge curve of $Li_2MnSiO_4$ and $Li_2Mn_{0.98}M_{0.02}SiO_4$ (M = Mg, Ni, Cr) samples at 0.1 C. The first discharge capacity of $Li_2MnSiO_4$, $Li_2Mn_{0.98}Mg_{0.02}SiO_4$, $Li_2Mn_{0.98}Ni_{0.02}SiO_4$, and $Li_2Cr_{0.98}M_{0.02}SiO_4$ is 12.2 mAh $g^{-1}$, 9.1 mAh $g^{-1}$, 8.5 mAh $g^{-1}$, and 29.8 mAh $g^{-1}$, respectively. It can be seen from the figure that the specific capacity of $Li_2Mn_{0.98}Mg_{0.02}SiO_4$ modified by $Mg^{2+}$ is not higher than that of the undoped sample. According to the research [21], $Mg^{2+}$ has good solubility, which can improve the stability of pure $P2_1/n$ structure. However, when the value of $x$ is in the range of 0.0–1.0, the substitution of Mg has no effect on the conductivity of electrons and ions.

The specific capacity of $Li_2Mn_{0.98}Ni_{0.02}SiO_4$ sample modified by $Ni^{2+}$ doping did not increase compared with the undoped sample. By referring to the literature [14, 22], we think that the reason for the poor electrochemical performance of Ni-doped samples is that almost all $Ni^{2+}$ is separated from the silicate structure. In addition, there is an optimal balance between Ni and $Ni^{2+}$, which has the best effect on improving the electrochemical performance. However, once the content of Ni exceeds or falls below a certain limit, the electrochemical performance will deteriorate. It can also be seen from the figure that the specific capacity of $Li_2Mn_{0.98}Cr_{0.02}SiO_4$ sample modified by $Cr^{3+}$ doping is higher than that of the undoped sample, and the voltage difference between charge and discharge is also reduced, indicating that adding Cr is conducive to improving conductivity, reducing cell polarization, and improving charge and discharge dynamic characteristics of the material. $Cr^{3+}$ is used to replace $Mn^{2+}$ in $Li_2MnSiO_4$. The ion radius of $Cr^{3+}$ (0.052 nm) is larger than that of $Mn^{2+}$ (0.046 nm). In the process of doping $Cr^{3+}$, with the increase of doping amount, the lattice gap is filled first, and then the conductivity will decrease. However, when it is increased to a certain extent, more and more lattice voids will be generated, which will provide better channels for the movement of electrons and ions, so as to improve the conductivity. Therefore, in the process of chromium doping, the electrochemical performance is the curve of decreasing and increasing cycle.

The electrochemical cycle performance of $Li_2MnSiO_4$ and $Li_2Mn_{0.98}M_{0.02}SiO_4$ (M = Mg, Ni, Cr) samples at 0.1 C is shown in Fig. 6. It can be seen from the figure that the discharge specific capacity of undoped samples and each doped sample decreases with the increase of cycle times.

Excluding Cr-doped sample, the cycle performance of Mg-doped and Ni-doped samples are lower than that of the undoped sample. This may be due to the fact that Mg doping has little effect on the performance of $Li_2MnSiO_4$ [21], while Ni has a multivalent state, which will cause lattice shrinkage in the process of charging and discharging, so it has a great influence on the structural stability of the material, and may lead to poor cycle performance. The first discharge specific capacity of $Li_2Mn_{0.98}Cr_{0.02}SiO_4$ can reach 29.8 mAh $g^{-1}$; after 70 cycles, it is 6.0 mAh $g^{-1}$; and its discharge retention rate is 20.1%. Because the bond energy of Cr-O (1086 kJ $mol^{-1}$) is greater than that of Mn-O (402 kJ $mol^{-1}$), the stability of $Li_2MnSiO_4$ structure can be enhanced by substituting Cr for Mn, and the cyclic performance of the material can be improved.

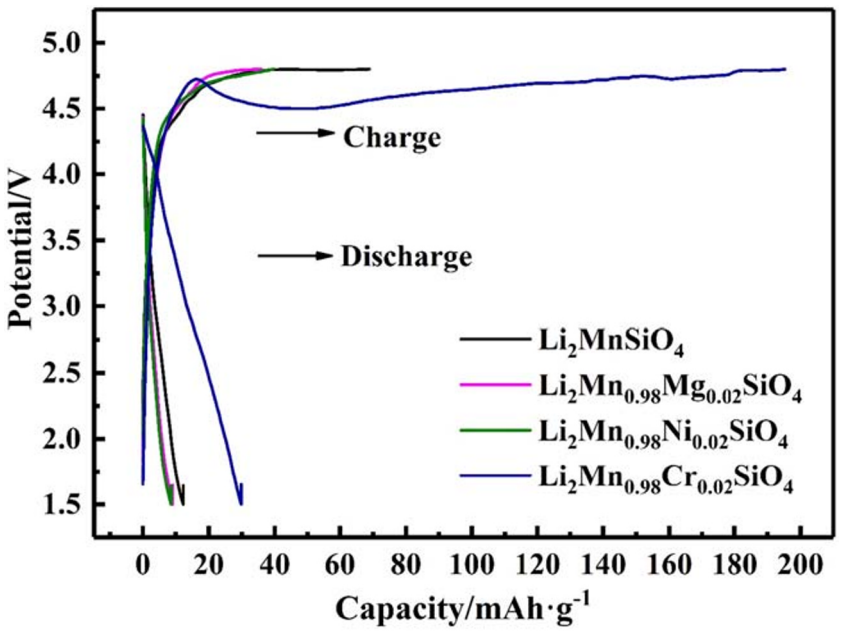


**Fig. 5** The first charge and discharge curve of $Li_2MnSiO_4$ and $Li_2Mn_{0.98}M_{0.02}SiO_4$ (M = Mg, Ni, Cr) samples at 0.1 C

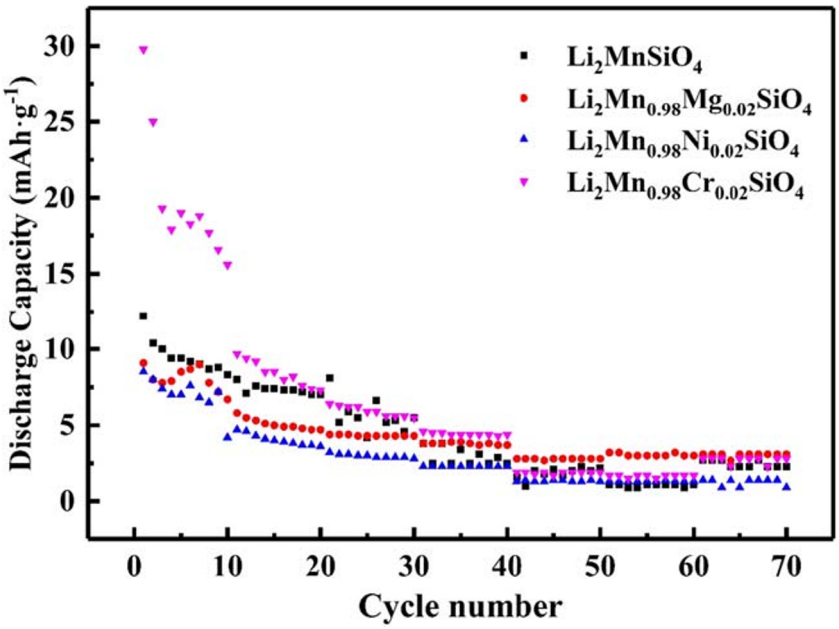


**Fig. 6** Electrochemical cycle curve of $Li_2MnSiO_4$ and $Li_2Mn_{0.98}M_{0.02}SiO_4$ (M = Mg, Ni, Cr) samples at 0.1 C

## Conclusions

Compared with $Li_2MnSiO_4$ sample, the electrochemical performance of $Li_2Mn_{0.98}Cr_{0.02}SiO_4$ synthesized by the solid-phase method is improved most obviously. Through XRD patterns, we can see that the second-phase $Li_{1.13}Mn_2O_4$ with good electrochemical performance is formed in the sample after Cr doping, which improves the electrochemical performance of the undoped sample. The primary particle size of Cr doped sample powder is smaller, which improves the diffusion ability of lithium-ion in $Li_2MnSiO_4$ crystal and contributes to the specific capacity of the material. In the process of $Cr^{3+}$ doping, the defect chemical mechanism changes with the increase of doping amount. The conductivity decreases first and then increases, which affects the electrical properties. At the same time, Cr-O bond energy is greater than Mn-O bond energy, and a proper amount of Cr replacing Mn can enhance the stability of $Li_2MnSiO_4$ structure, thus improving the cyclic performance of the material. The improvement of $Li_2Mn_{0.8}Cr_{0.2}SiO_4$ is the most obvious, the first discharge capacity is 29.8 mAh $g^{-1}$, the discharge capacity after 70 cycles is 6 mAh $g^{-1}$, and the capacity retention rate is 20.1%.

**Funding information** This work was financially supported by the National Natural Science Foundation of China (Nos. 51874079, 51674068, 51804035); the Natural Science Foundation of Hebei Province (No. E2018501091); the Training Foundation for Scientific Research of Talents Project, Hebei Province (No. A2016005004); the Fundamental Research Funds for the Central Universities (Nos. N172302001, N182312007, N182306001, N2023040); and the Hebei Province Key Research and Development Plan Project (No. 19211302D).

## References

1. Li J, Luo S, Ding X, Wang Q, He P (2018) Three-dimensional honeycomb-structural LiAlO2-modified LiMnPO4 composite with superior high rate capability as Li-ion battery cathodes. ACS Appl Mater Inter 10(13):10786–10795. https://doi.org/10.1021/acsami.7b17597
2. Liu C, Luo S, Huang H, Wang Z, Wang Q, Zhang Y, Liu Y, Zhai Y, Wang Z (2018) Potassium vanadate K0.23V2O5 as anode materials for lithium-ion and potassium-ion batteries. J Power Sources 389:77–83. https://doi.org/10.1016/j.jpowsour.2018.04.014
3. Liu H, Luo S, Yan S, Wang Q, Hu D, Wang Y, Feng J, Yi T (2019) High-performance α-Fe2O3/C composite anodes for lithium-ion batteries synthesized by hydrothermal carbonization glucose method used pickled iron oxide red as raw material. Compos Part B Eng 164:576–582. https://doi.org/10.1016/j.compositesb.2019.01.084
4. Effect of structure on the Fe3 + / Fe2 + redox couple in iron phosphates
5. Arroyo-de Dompablo ME, Armand M, Tarascon JM, Amador U (2006) On-demand design of polyoxianionic cathode materials based on electronegativity correlations: An exploration of the Li2MSiO4 system (M=Fe, Mn, Co, Ni). Electrochem Commun 8(8):1292–1298. https://doi.org/10.1016/j.elecom.2006.06.003
6. Dominko R, Bele M, Gaberšček M, Meden A, Remškar M, Jamnik J (2006) Structure and electrochemical performance of Li2MnSiO4 and Li2FeSiO4 as potential Li-battery cathode materials. Electrochem Commun 8(2):217–222. https://doi.org/10.1016/j.elecom.2005.11.010
7. Qiu S, Pu X, Ai X, Yang H, Chen Z, Cao Y (2018) Template synthesis of mesoporous Li2MnSiO4@C composite with improved lithium storage properties. Electrochim Acta 291:124–131. https://doi.org/10.1016/j.electacta.2018.08.146
8. Shree Kesavan K, Michael MS, Prabaharan SRS (2019) Facile electrochemical activity of monoclinic Li2MnSiO4 as potential cathode for Li-ion batteries. ACS Appl Mater Inter 11(32):28868–28877. https://doi.org/10.1021/acsami.9b08213
9. Yan X, Hou Y, Huang Y, Zheng S, Shi Z, Tao X (2019) Effects of Ga, Ge and As modification on structural, electrochemical and

electronic properties of Li2MnSiO4. J Electrochem Soc 166(15): A3874–A3880. https://doi.org/10.1149/2.1321915jes
10. Dominko R, Bele M, Kokalj A, Gaberscek M, Jamnik J (2007) Li2MnSiO4 as a potential Li-battery cathode material. J Power Sources 174(2):457–461. https://doi.org/10.1016/j.jpowsour.2007.06.188
11. Zhu H, Deng W, Chen L, Zhang S (2019) Nitrogen doped carbon layer of Li2MnSiO4 with enhanced electrochemical performance for lithium ion batteries. Electrochim Acta 295:956–965. https://doi.org/10.1016/j.electacta.2018.11.133
12. Wang C, Xu Y, Sun X, Zhang B, Chen Y, He S (2018) Enhanced electrochemical properties of F-doped Li2MnSiO4/C for lithium ion batteries. J Power Sources 378:345–352. https://doi.org/10.1016/j.jpowsour.2017.12.004
13. Modification and deterioration mechanism of lithium manganese silicate as cathode material for lithium-ion batteries. https://doi.org/10.7521/j.issn.0454-5648.2013.10.14
14. Effect of Ni substitution on structural stability, micromorphology, and electrochemical performance of Li2MnSiO4/C cathode materials
15. Cheng H, Zhao S, Wu X, Zhao J, Wei L, Nan C (2018) Synthesis and structural stability of Cr-doped Li 2 MnSiO 4/C cathode materials by solid-state method. Appl Surf Sci 433:1067–1074. https://doi.org/10.1016/j.apsusc.2017.10.045
16. Spectrochim Acta A Mol Biomol Spectrosc. https://doi.org/10.1016/j.saa.2014.02.095
17. Wei Y, Wang LJ, Yan J et al (2011) Calcination temperature effects on the electrochemical performance ofLi2MnSiO4/C cathode material for Lithium ion batteries. Acta Phys -Chim Sin 27(11): 2587–2592
18. Duncan H, Kondamreddy A, Mercier PHJ, Le Page Y, Abu-Lebdeh Y, Couillard M, Whitfield PS, Davidson IJ (2011) Novel Pn polymorph for Li2MnSiO4 and its electrochemical activity as a cathode material in Li-ion batteries. Chem Mater 23(24):5446–5456. https://doi.org/10.1021/cm202793j
19. Liu C, Luo S, Huang H, Zhai Y, Wang Z (2019) Layered potassium-deficient P2- and P3-type cathode materials KxMnO2 for K-ion batteries. Chem Eng J 356:53–59. https://doi.org/10.1016/j.cej.2018.09.012
20. Zhou LZ, Xu QJ, Liu MS, Jin X (2013) Novel solid-state preparation and electrochemical properties of Li1.13[Ni0.2Co0.2Mn0.47]O2 material with a high capacity by acetate precursor for Li-ion batteries. Solid State Ionics 249-250: 134–138. https://doi.org/10.1016/j.ssi.2013.07.024
21. Arsentev M, Hammouri M, Kovalko N, Kalinina M, Petrov A (2017) First principles study of the electrochemical properties of Mg-substituted Li2MnSiO4. Comp Mater Sci 140:181–188. https://doi.org/10.1016/j.commatsci.2017.08.045
22. Saracibar A, Wang Z, Carroll KJ, Meng YS, Dompablo MEA (2015) New insights into the electrochemical performance of Li2MnSiO4: effect of cationic substitutions. J Mater Chem A 3(11):6004–6011. https://doi.org/10.1039/C4TA03367A